

Biospecific Binding of Carbonic Anhydrase to Mixed SAMs Presenting Benzenesulfonamide Ligands: A Model System for Studying Lateral Steric Effects

Joydeep Lahiri, Lyle Isaacs,[†] Bartosz Grzybowski, Jeffrey D. Carbeck,[‡] and George M. Whitesides*

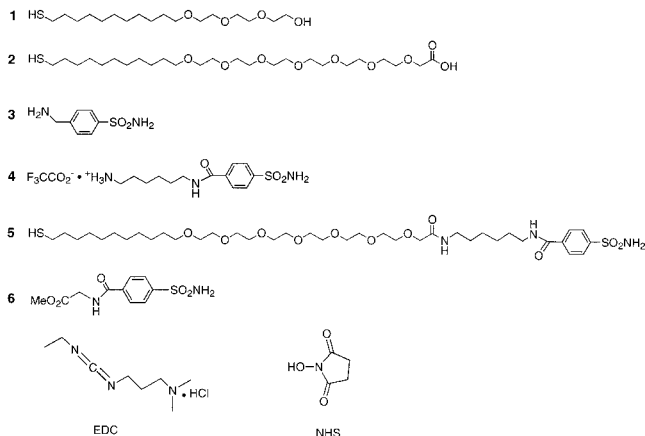
Department of Chemistry and Chemical Biology, Harvard University, 12 Oxford Street, Cambridge, Massachusetts 02138

Received October 13, 1998. In Final Form: June 23, 1999

This work describes the binding of carbonic anhydrase (CA) to mixed self-assembled monolayers (SAMs) presenting benzenesulfonamide ligands at a surface consisting primarily of tri(ethylene glycol) [(EG)₃OH] groups. Surface plasmon resonance (SPR) quantified the binding of CA to the benzenesulfonamide groups. Two factors influenced the binding of CA: (a) the density of benzenesulfonamide groups at the surface, and (b) the coverage of the surface with molecules of CA adsorbed to these benzenesulfonamide groups. At low mole-fractions of benzenesulfonamide groups in the mixed SAM where the binding of CA is highly (>90%) reversible, we observe: (a) an approximately 10-fold decrease in the observed bimolecular rate constant for association, $k_{\text{on,obs}}$, during the binding of CA (as the fraction of the surface covered by adsorbed CA increases from ~0.15 to ~0.35, the value of $k_{\text{on,obs}}$ decreases from $\sim 40 \times 10^3 \text{ M}^{-1} \text{ s}^{-1}$ to $\sim 4 \times 10^3 \text{ M}^{-1} \text{ s}^{-1}$); (b) almost no corresponding changes in the observed unimolecular rate constant for dissociation ($k_{\text{off,obs}} \sim 0.005 \text{ s}^{-1}$) during the dissociation of CA from the surface. These observations establish that $k_{\text{on,obs}}$ is influenced by the extent of coverage of the surface with CA, but that $k_{\text{off,obs}}$ is not. At low surface densities of arylsulfonamide groups, one hypothesis that rationalizes these data is that the decrease in $k_{\text{on,obs}}$ reflects repulsive steric interactions between molecules of CA near the surface and those already adsorbed. Each molecule of biospecifically adsorbed CA shields proximal benzenesulfonamide ligands from binding to incoming molecules of CA, and decreases the surface density of these ligands that are accessible to CA, at a rate that increases nonlinearly with the quantity of CA already adsorbed.

Introduction

Our objective in this work was to investigate lateral steric interactions—that is, interactions between molecules of protein associated with the surface, or in solution but close enough to the surface to interact with associated molecules—during binding of proteins to ligands immobilized at surfaces. These surfaces consisted of self-



assembled monolayers (SAMs) of alkanethiolates on gold-presenting benzenesulfonamide (ASA, arylsulfonamide)

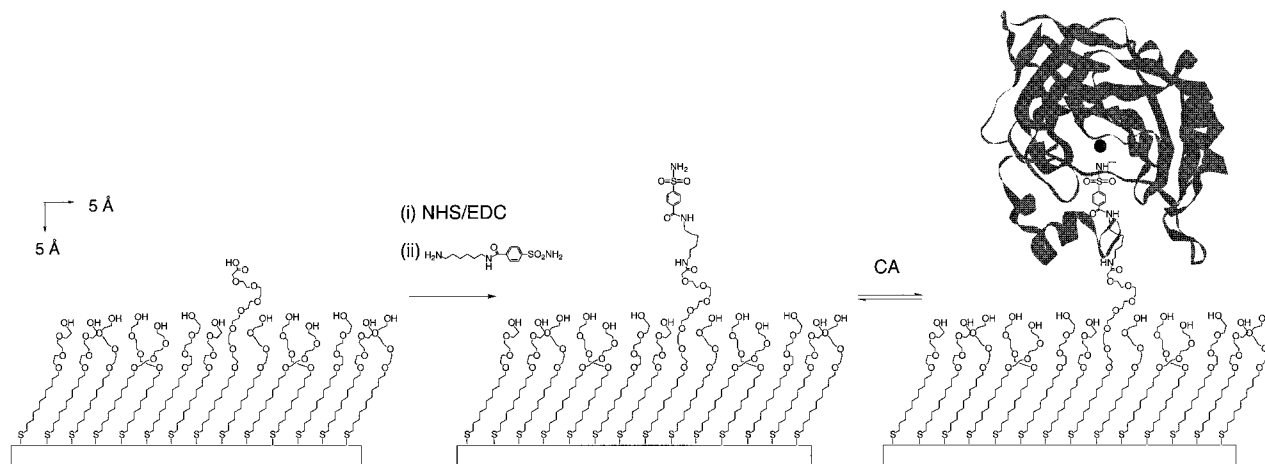
* Corresponding author: phone (617) 495 9430; fax (617) 495 9857.

[†] Current address: Department of Chemistry and Biochemistry University of Maryland at College Park, College Park, MD 20742.

[‡] Current address: Department of Chemical Engineering, Princeton University, Princeton, NJ 08544.

groups and tri(ethylene glycol) [(EG)₃OH] groups (Scheme 1). We studied the binding of carbonic anhydrase (CA) to these surfaces using surface plasmon resonance (SPR). This report describes the influence of two factors on the kinetics of binding of CA to mixed SAMs: (a) the density of ASA groups immobilized at the surface, and (b) the density of molecules of CA adsorbed to these ASA groups. The most important observations are: (a) at very low surface densities of ASA groups [$\chi(\text{ASA}) < 0.005$], the binding is well-described by single values of rate constants of association and dissociation; (b) at low surface densities of ASA groups [$0.005 < \chi(\text{ASA}) < 0.05$] where the binding is still highly reversible, the observed bimolecular rate constant for association ($k_{\text{on,obs}}$) decreases as the quantity of CA adsorbed on ASA groups at the surface increases (we observe a 10-fold decrease in $k_{\text{on,obs}}$ as the fraction of the surface covered by adsorbed CA increases from ~0.15 to ~0.35); and (c) at these surface densities of ASA groups, the observed unimolecular rate constant for dissociation ($k_{\text{off,obs}}$) is not influenced by adsorbed CA.

An experimental model system to study fundamental aspects of biomolecular recognition at surfaces must include at least three components: (a) a model surface that is well-defined on a molecular scale; (b) a recognition event that is not complicated by processes that may occur during binding at surfaces (for example, an equilibrium binding constant whose strength depends on multivalent binding, or rate constants influenced by mass transport or rebinding), and (c) an analytical technique that permits convenient collection of relevant data. In studying the effects of lateral interactions on the binding of proteins to surfaces, we have chosen to work with a system

Scheme 1. Binding of CA to Mixed SAMs Presenting Benzenesulfonamide Ligands (4)^a

^a The ligand is covalently immobilized to the surface by amide bond-forming reactions between its terminal amino group and active (NHS) esters on the SAM. The components of the system are drawn to scale.

Table 1. Thermodynamic and Kinetic Constants for Binding of CA to ASA Ligands

	technique	k_{on} ($10^4 \text{ M}^{-1} \text{ s}^{-1}$)	k_{off} (10^{-3} s^{-1})	K_d (μM)	reference
1 R = $-\text{COO}^-$	ACE			2.2	40
2 R = $-\text{CONHCH}_2\text{CH}_3$	fluorescence	86	25	0.029	13
3 R = $-\text{CONHCHCOO}^-$ CHCH ₃ CH ₂ CH ₃	fluorescence	220	11	0.0050	12
4 R = $-\text{CONHCH}_2\text{COO}^-$	fluorescence	36	120	0.33	12
5 R = $-\text{H}$	ACE	11	100	0.91	42
	kinetics ^c	10	44	0.44	43
6 R = $-\text{CONH}(\text{CH}_2)_6\text{NHCO}(\text{EG})_6^b$ (5)	SPR	1.9	5.4	0.26	1
7 ^a R = $-\text{CONH}(\text{CH}_2)_6\text{NHCO}(\text{EG})_6^b$ $\chi(2/4) \approx 0.02$	SPR	3.5 ^d 0.42 ^e	5.3 5.3	0.15 1.3	

^a Entry 7 corresponds to values of k_{on} and k_{off} determined by SPR in this paper. ^b The hexa(ethylene glycol) moiety was attached to SAMs of alkanethiolates on gold. ^c Values of kinetic constants were obtained by kinetic studies of inhibition of CO_2 hydration by CA. ^{d,e} The values correspond to fractional coverages (P/P_{max}^{st}) of 0.15 and 0.35, respectively (see Figure 7).

composed of SAMs of alkanethiolates on gold, the CA-ASA interaction, and SPR.

Mixed SAMs of Alkanethiolates on Gold as Model Surfaces for Studies of Biomolecular Recognition.

Mixed SAMs of alkanethiolates on gold presenting well-defined amounts of a ligand at an interface that otherwise consists of tri(ethylene glycol) groups satisfy three requirements:¹⁻⁸ (a) they resist nonspecific adsorption of biomolecules, (b) they are easily modified synthetically to include delicate and complex functional groups, and (c) they can be prepared in ways that control the average surface density of ligands used for biospecific binding.

CA-ASA Interaction. The carbonic anhydrases are a well-characterized group of enzymes that bind para-

substituted ASAs with dissociation constants (K_d) in the range 10^{-6} – 10^{-9} M.⁹ The reported values (from studies in solution) of k_{on} are $\sim 10^5$ – $10^7 \text{ M}^{-1} \text{ s}^{-1}$; values for k_{off} are $\sim 10^{-2}$ – 10^{-1} s^{-1} (also see Table 1 in *Discussion*).⁹⁻¹² ASAs bind to CA by coordination of the sulfonamide ($-\text{SO}_2\text{NH}_2$) moiety as an anion (SO_2NH^-) to a zinc ion located at the bottom of a conical cleft in the enzyme that is roughly 15 Å deep.⁹ We have demonstrated that bovine CA undergoes biospecific adsorption to mixed SAMs presenting ASA ligands (5) at a surface composed primarily of tri(ethylene glycol) groups,¹ and monitored in situ by SPR. At the low mole fractions of ASA used in the reported study ($\chi_{ASA} \leq 0.05$), the adsorption of CA was $\sim 90\%$ reversible. The reversibility of this association makes the ASA-CA interaction an attractive model system with which to study binding of proteins at surfaces. The kinetic constants reported (using SPR) by Mrksich et al. for binding of bovine CA (from bovine erythrocytes, containing A and B

(1) Mrksich, M.; Grunwell, J. R.; Whitesides, G. M. *J. Am. Chem. Soc.* **1995**, *117*, 12009–12010.

(2) Mrksich, M.; Whitesides, G. M. *Annu. Rev. Biophys. Biomol. Struct.* **1996**, *25*, 55–78.

(3) Mrksich, M. *Curr. Opin. Colloid Interface Sci.* **1997**, *2*, 83–88.

(4) Mrksich, M.; Whitesides, G. M. In *Poly(ethylene glycol) Chemistry and Biological Applications*; Harris, J. M.; Zalipsky, S., Eds.; American Chemical Society: Washington, DC, 1997; Vol. 680, pp 361–373.

(5) Sigal, G. B.; Bamdad, C.; Barberis, A.; Strominger, J.; Whitesides, G. M. *Anal. Chem.* **1996**, *68*, 490–497.

(6) (a) Lahiri, J.; Isaacs, L.; Tien, J.; Whitesides, G. M. *Anal. Chem.* **1999**, *71*, 777–790. (b) Lahiri, J.; Ostuni, E.; Whitesides, G. M. *Langmuir* **1999**, *6*, 2055–2060.

(7) Prime, K. L.; Whitesides, G. M. *Science* **1991**, *252*, 1164–1167.

(8) Prime, K. L.; Whitesides, G. M. *J. Am. Chem. Soc.* **1993**, *115*, 10714–10721.

(9) Dodgson, S. J.; Tashian, R. E.; Gros, G.; Carter, N. D. *The Carbonic Anhydrases: Cellular Physiology and Molecular Genetics*; Plenum Press: New York, 1991.

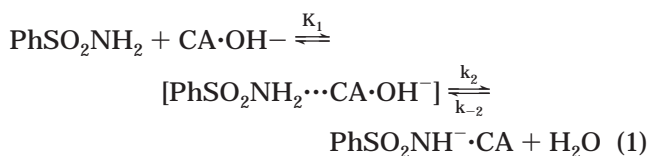
(10) Taylor, P. W.; King, R. W.; Burgen, A. S. V. *Biochemistry* **1970**, *9*, 3894–3902.

(11) Taylor, P. W.; King, R. W.; Burgen, A. S. V. *Biochemistry* **1970**, *9*, 2638–2645.

(12) Sigal, G. B.; Whitesides, G. M. *Bioorg. Med. Chem. Lett.* **1996**, *6*, 559–564.

isozymes) to mixed SAMs consisting of **1** and **5** were: $k_{on} \approx 1.9 \times 10^4 \text{ M}^{-1} \text{ s}^{-1}$, $k_{off} \approx 5 \times 10^{-3} \text{ s}^{-1}$, $K_d \approx 3 \times 10^{-7} \text{ M}$.

Taylor et al.^{11,13} proposed a two-step mechanism for binding of ASA to CA: a partitioning of the ASA group into the active site, driven primarily by hydrophobic interactions, followed by coordination of the weakly associated ASA group to the zinc ion in the active site to give the final complex (eq 1). This mechanism is based on four



observations: (a) there is a strong correlation between k_{on} and the octanol–water partition coefficients of substituted ASAs;¹³ this correlation is also observed for binding of substituted ASAs to apocarbonic anhydrase [apo-CA, the protein lacking an active site Zn(II)];¹³ (b) the rate of binding of ASA groups to apo-CA is not influenced by pH but the rate of binding of ASA to CA is influenced by pH;¹³ (c) the kinetics of binding of ASA to CA is well-described by *single observable rate constants* for association (k_{on}) and dissociation (k_{off}); this observation indicates that the partitioning of ASA (between aqueous solvent and the hydrophobic active site of CA) is fast compared with formation and cleavage of the sulfonamide–zinc bond; that is, $k_{on} \approx K_1 k_2$ and $k_{off} \approx k_{-2}$; (d) the total charge of the CA·ASA complex is the same as that of CA in the absence of ASA (see *Discussion*); therefore the water molecule coordinated to the Zn(II) ion exists primarily as a hydroxide ion.

Surface Plasmon Resonance. SPR measures the intensity of reflection of monochromatic p-polarized light incident on the back side of a gold-coated glass slide. Changes in the angle θ_m at which the intensity of reflected light is at a minimum are related to changes in index of refraction in the region near the gold–solution interface [within approximately one-quarter wavelength ($\sim 200 \text{ nm}$) of the incident light].^{14,15} Within a family of similar compounds (e.g., proteins), changes in θ_m correlate linearly with the mass per unit area of protein adsorbed.^{16,17} The BIAcore instrument (used in this study) reports changes in θ_m in resonance units (RU; $10\,000 \text{ RU} = 1^\circ$). For most proteins, a change in θ_m of 1000 RU corresponds to a change of about 1 ng/mm^2 in the quantity of protein adsorbed at the surface.¹⁸

A typical binding experiment using SPR has three phases (Figure 1): (a) a buffer (e.g., phosphate buffered saline, PBS) is passed over the sensing surface; (b) the buffer is changed to a solution containing the analyte; and (c) the solution is then replaced by the original buffer. There is a rapid increase in response (as observed by an increase in RU) upon introduction of the solution of the protein; this immediate response (within $\sim 2 \text{ s}$, at a flow rate of $10 \mu\text{L min}^{-1}$) reflects the change in the bulk

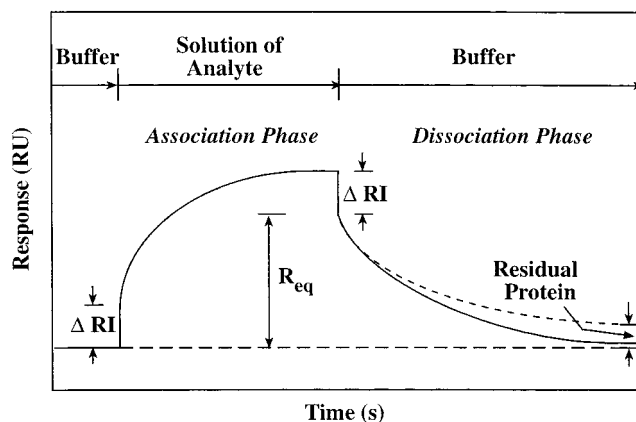


Figure 1. SPR sensorgrams showing various stages of association of a protein with a ligand on the surface, and of dissociation of the protein–ligand complex. The two sensorgrams have identical rates of association, but differ in the extent of reversibility of binding. ΔRI refers to the change in the bulk refractive index when the solution of buffer is replaced by the solution of protein, and R_{eq} is the equilibrium response.

refractive index (labeled ΔRI in Figure 1) between the buffer and the solution of protein. This fast change is followed by a slower increase in response due to adsorption of the protein at the interface. At equilibrium, when the net rate of binding to the surface is zero, the response reaches a plateau. It is possible to estimate the amount of protein adsorbed at equilibrium (R_{eq}) by subtracting the response due to the refractive index change (ΔRI) from the response at equilibrium. When the protein solution is replaced by the original PBS buffer, there is an initial fast drop in response resulting from the differences in the index of refraction of the two solutions, followed by a slower decrease in the response due to desorption of the analyte. If the response during the desorption phase does not reach the value preceding injection of the protein, there is still some protein adsorbed to the surface; this residual protein could be irreversibly adsorbed or undergo slow dissociation that is incomplete in the time scale of the SPR experiment. We refer to the adsorption of the analyte (CA, in this paper) to ligands (ASA groups, in this paper) presented at the surface as the “association phase” and the desorption of the analyte from the surface as the “dissociation phase”.

The BIAcore 1000 is well-suited for binding studies in which the rate constants of binding are in the range described in this report ($k_{on,obs} \sim 10^4\text{--}10^3 \text{ M}^{-1} \text{ s}^{-1}$, $k_{off,obs} \sim 0.005 \text{ s}^{-1}$). The range of relevant rates was an important factor in choosing the CA-ASA interaction as a model system to investigate the effects of lateral interactions on processes occurring at interfaces.

Previous Work on Lateral Steric Effects. The influence of steric effects during adsorption phenomena involving macromolecules (e.g., protein, DNA)^{19–22} or self-assembled structures (e.g., vesicles)²³ has been described. Biospecific binding of proteins to ligands at surfaces has been investigated by several researchers, for example, by Tamm and Bartoldus in phosphatidylcholine vesicles,¹⁹ by Edwards et al. in dextran,²⁰ and by Spinke et al. in SAMs of alkanethiolates on gold.²¹ Tamm and Bartoldus

(13) King, R. W.; Burgen, A. S. V. *Proc. R. Soc. London Ser. B* **1976**, *193*, 107–125.

(14) Raether, H. *Phys. Thin Films* **1977**, *9*, 145–261.

(15) Kretschmann, E.; Raether, H. *Z. Naturforsch. A: Astrophys., Phys., Chem.* **1968**, *23*, 2135.

(16) Fagerstam, L. G.; Frostell-Karlsson, Å.; Karlsson, R.; Persson, B.; Ronnberg, I. *J. Chromatogr.* **1992**, *597*, 397–410.

(17) Chaiken, I.; Rose, S.; Karlsson, R. *Anal. Biochem.* **1991**, *201*, 197–210.

(18) Stenberg, E.; Person, B.; Roos, H.; Urbaniczky, C. *J. Colloid Interface Sci.* **1991**, *143*, 513–526.

(19) Tamm, L. K.; Bartoldus, I. *Biochemistry* **1988**, *27*, 7453–7458.

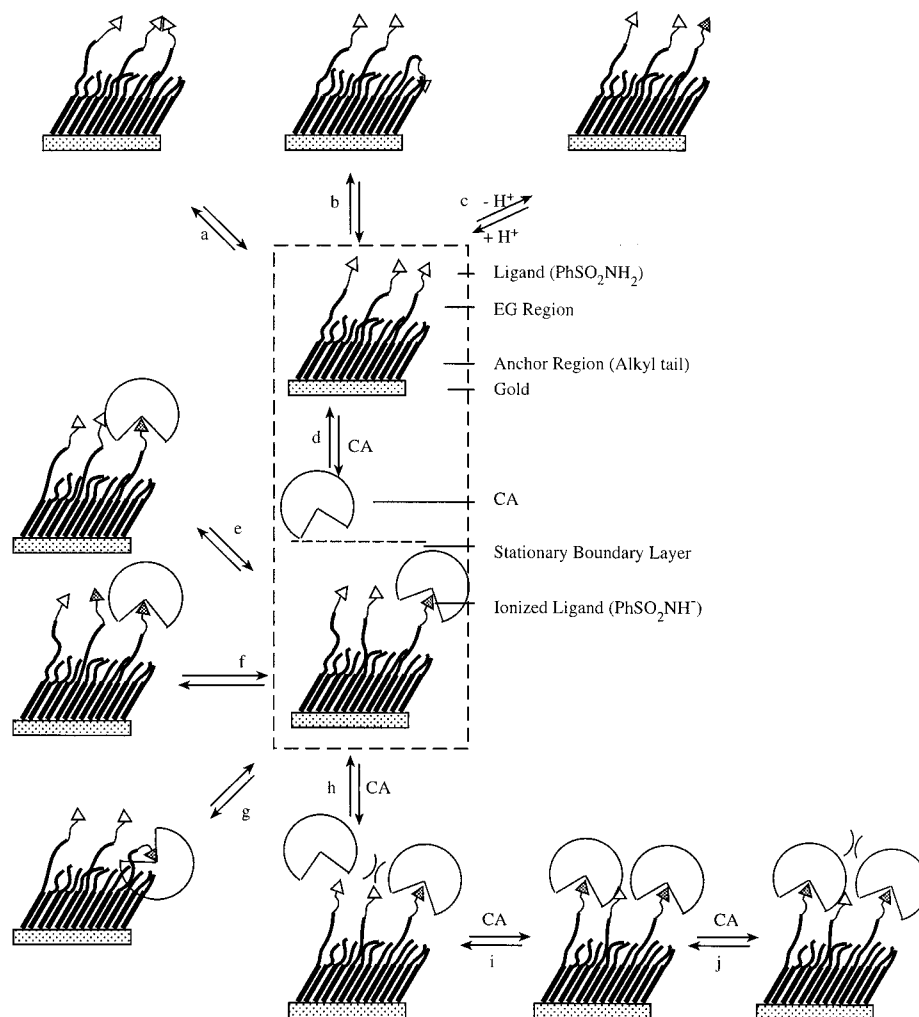
(20) Edwards, P. R.; Gill, A.; Pollard-Knight, D. V.; Hoare, M.; Buckle, P. E.; Lowe, P. A.; Leatherbarrow, R. *J. Anal. Biochem.* **1995**, *231*, 210–217.

(21) Spinke, J.; Liley, M.; Schmitt, F.-J.; Guder, H.-J.; Angermaier, L.; Knoll, W. *J. Chem. Phys.* **1993**, *99*, 7012–7019.

(22) Berg, O. G. *Makromol. Chem.* **1988**, *17*, 161–175.

(23) Jones, M. N. *Curr. Opin. Colloid Interface Sci.* **1996**, *1*, 91–100.

Scheme 2. Schematic Representation of Various Processes that Might Occur at the Surface during Binding of CA to ASA Groups on the SAM^a



^a The dashed box in the center shows the transport of molecules of CA from bulk solution to the stationary boundary layer in contact with the SAM and the binding of CA to ASA groups (d). Some other possible processes are: (a) two proximate ASA groups might dimerize; association with CA would require dissociation of this dimer. (b) An ASA group might associate with the (EG)₃ layer; association with CA would again require dissociation. (c) Ionization of the ASA group to form the anion might be influenced by the lower (relative to bulk buffer) dielectric constant of the interface. (e) Secondary nonspecific binding of adsorbed CA to a proximate ASA ligand might influence the extent of reversibility and also prevent the binding of another molecule of CA to the proximate ligand. (f) Adsorbed molecules of CA might change the local dielectric constant and decrease the propensity for ionization of ASA groups; a decrease in the extent of ionization would decrease the value of the observed rate constant for association. (g) The adsorbed molecule of CA might associate with the (EG)₃ layer; this association might influence the reversibility of binding. (h) Molecules of CA might be sterically hindered from binding to an ASA ligand because of proximate ASA groups. (i and j) Molecules of adsorbed CA might shield proximate ASA groups and decrease the number of free ASA groups available for binding; this shielding would result in a decrease in the observed rate constant for association.

and Edwards et al. studied the binding of antibodies to antigens. In both these studies, the binding was not adequately described by simple kinetic models and deviations were attributed to lateral steric effects. There are additional complications in studies of the kinetics of binding of antibodies to surfaces because of the influence of bivalency, and because the rapid binding of antibodies to antigen ($k_{\text{on}} \sim 10^6\text{--}10^7 \text{ M}^{-1} \text{ s}^{-1}$)^{24–26} makes the overall rate of association limited by the rate of mass transport of protein molecules from the bulk solution through the unstirred boundary layer to the surface. Spinke et al. studied the binding of streptavidin to SAMs presenting biotin groups. In this study, they observed that maximal

binding of streptavidin occurred in mixed monolayers in which the biotin ligand had an appropriate spacer and was present at low surface densities. The interaction of streptavidin to biotin is essentially irreversible and therefore not amenable to estimations of k_{on} and k_{off} . In this report, we describe steric effects during the reversible and monovalent binding of CA to ASA groups on a surface that is resistant to nonspecific adsorption.

A central observation of this paper is that $k_{\text{on,obs}}$ (but not $k_{\text{off,obs}}$) decreases as the coverage of the surface by molecules of CA increases. An analysis of this observation requires an understanding of the system (Scheme 2). Some of the issues that are relevant to biospecific binding of proteins to SAMs are shown schematically in Scheme 2, and a discussion of lateral effects and alternative explanations that might account for the observations described in the paper are presented in the *Discussion*.

(24) Glaser, R. W. *Anal. Biochem.* **1993**, *213*, 152–161.

(25) Myszkowski, D. G.; Morton, T. A.; Doyle, M. L.; Chaiken, I. M. *Biophys. Chem.* **1997**, *64*, 127–137.

(26) Johne, B.; Gadnell, M.; Hansen, K. *J. Immunol. Methods* **1993**, *160*, 191–198.

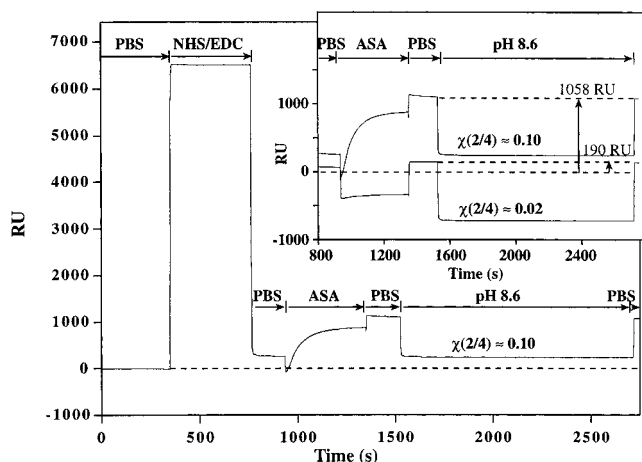


Figure 2. SPR sensorgrams showing coupling of the ASA ligand, **4**, to mixed SAMs consisting of **1** and **2**, with $\chi(2) \approx 0.10$. The surface, after being equilibrated with PBS, was treated sequentially with an aqueous solution containing NHS (0.05 M) and EDC (0.20 M), a phosphate-buffered solution of **4** (2 mg mL⁻¹, pH 8), and pH 8.6 phosphate buffer (25 mM). The surface was washed with PBS after each injection. The inset shows the relative amounts of immobilization on SAMs with $\chi(2) \approx 0.10$ (≈ 1058 RU) and $\chi(2) \approx 0.02$ (≈ 190 RU).

Results

Preparation of SAMs Presenting ASA Ligands. The commercially available sensor chip for SPR consists of a layer of carboxymethyl dextran (~ 100 nm thick) covalently attached to a hydroxy-terminated alkanethiol monolayer on gold. To avoid kinetic and thermodynamic problems resulting from the requirement that the protein must partition into the gel layer to reach the ligand, we used a surface consisting only of mixed SAMs of alkanethiolates of **1** and **2** on gold, and coupled ligands to the carboxylic acid groups of **2** by peptide bond-forming reactions (Scheme 1).^{1,6} These purely SAM-based chips have several advantages over the dextran gel-based chips: (a) there is almost no detectable nonspecific adsorption of proteins on SAMs consisting of **1** and **2** (the amount of nonspecific adsorption on the carboxylated dextran gel is significant);⁶ (b) the density of ligands at the surface in chips made from **1** and **2** can be easily manipulated by varying the ratio of **1** to **2**; control of the density of ligands in the dextran gel requires manipulation of the pH of coupling, and the use of auxiliary nucleophiles (e.g., ethanolamine); (c) in mixed SAMs consisting of **1** and derivatives of **2**, binding occurs at the surface of the SAM; although mass transport may influence the kinetics of binding, the system is otherwise uncomplicated. In the gel, bulky molecules of analyte must first partition into the dextran gel, and equilibrate by diffusing through the relatively thick cross-linked gel layer, before binding to ligands inside the gel.

The couplings of the ASA ligands to the mixed SAM were conducted inside the SPR instrument⁶ by sequential injections of an aqueous solution containing *N*-hydroxysuccinimide (NHS) (0.05 M) and 1-(3-dimethylamino-propyl)-3-ethylcarbodiimide hydrochloride (EDC) (0.20 M) (to transform the surface carboxylic acid groups into activated NHS esters), and then a solution of the ligand (2 mg mL⁻¹; 25 mM pH 8 phosphate buffer). The surface was washed with PBS after each injection; unreacted NHS esters were hydrolyzed by washing the surface with pH 8.6 phosphate buffer. Figure 2 is an SPR sensorgram showing the immobilization of **4** to a mixed SAM with the mole fraction of **2** [$\chi(2)$] ≈ 0.10 . The inset in Figure 2 shows the relative amounts of immobilization (of **4**) on two

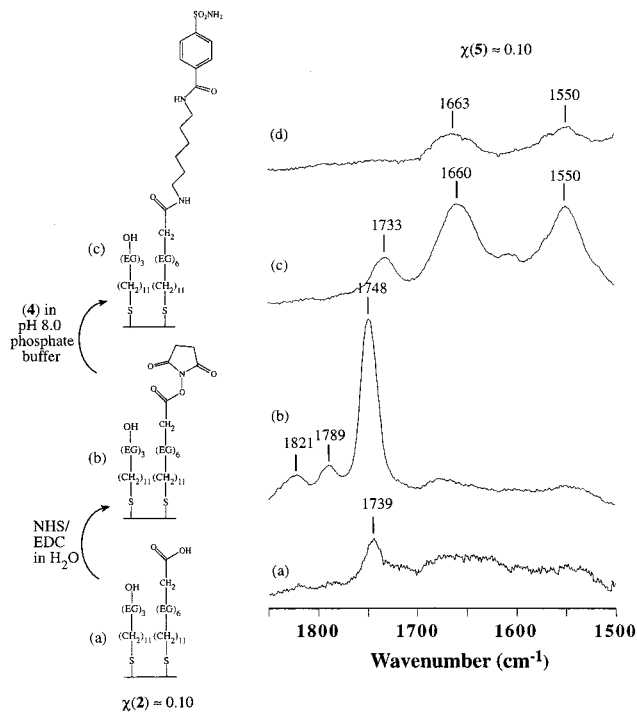


Figure 3. Schematic representation and PIERS spectra (of the C=O region) showing the formation of the NHS ester of **2** in mixed SAMs consisting of **1** and **2** [$\chi(2) \approx 0.10$], and the subsequent reaction of the NHS ester with **4**. The PIERS spectra of the mixed SAM with $\chi(2) \approx 0.10$, equilibrated with PBS, rinsed with water and ethanol, and dried under a stream of nitrogen is shown in (a). Treatment of this SAM with an aqueous solution of NHS and EDC (see text and *Experimental Section* for details), followed by brief rinsing (water and ethanol), and drying under nitrogen results in a SAM whose PIERS spectra is shown in (b). Treatment of the activated SAM with an aqueous solution of **4**, followed by rinsing (water, ethanol) and drying with nitrogen, results in a SAM whose spectra is shown in (c). Trace (d) shows PIERS spectra of a mixed SAM consisting of **1** and **5** [$\chi(5) \approx 0.10$].

different mixed SAMs with $\chi(2) \approx 0.10$ and 0.02 —the amount of ligand immobilized on the SAM with $\chi(2) \approx 0.10$ (1058 RU, i.e., 1.058 ng mm⁻²) is approximately five times that on the SAM with $\chi(2) \approx 0.02$ (190 RU, i.e., 0.190 ng mm⁻²).

We used polarized infrared external reflectance spectroscopy (PIERS) to study the coupling of **4** to the mixed SAMs. PIERS provides information about the presence of functional groups that are detectable by IR, and also about the order and orientation of the hydrocarbon chains within a SAM.²⁷ In PIERS, vibrational modes with transition dipole moments perpendicular to the surface show maximal absorbances; vibrational modes with transition dipole moments parallel or nearly parallel to the surface show zero or minimal absorbances.²⁸ Figure 3 shows PIERS spectra of the mixed SAMs [$\chi(2) \approx 0.10$] in the carbonyl (C=O) stretching region before activation with NHS/EDC (a), after activation with NHS/EDC (b), and after coupling to **4** (c). We assign the band centered at 1739 cm⁻¹ to the C=O stretch of the carboxylic acid groups in **2**. After treatment of the SAM with NHS/EDC, three new bands at 1748, 1789, and 1821 cm⁻¹ appear in the spectrum. On the basis of assignments by Frey and Corn²⁹ for NHS esters of SAMs, we assign the peak at 1748 cm⁻¹ to an asymmetric stretch of the NHS carbonyls, the peak at 1789 cm⁻¹ to

(27) Porter, M. D. *Anal. Chem.* **1988**, *60*, 3187–3193.

(28) Greenler, R. G. *J. Phys. Chem.* **1966**, *44*, 310–315.

(29) Frey, B. L.; Corn, R. M. *Anal. Chem.* **1996**, *68*, 3187–3193.

a symmetric stretch of the NHS carbonyls, and the peak at 1821 cm^{-1} to the carbonyl stretch of the NHS ester of **2**. Upon treatment of the activated SAM with a solution containing **4** (2 mg mL^{-1}), the bands due to the NHS esters disappear, and three bands centered at 1550 , 1660 , and 1733 cm^{-1} appear. A mixed SAM consisting of **1** and **5** also shows bands of approximately equal intensity at 1550 and 1660 cm^{-1} ; on the basis of these observations, we conclude that the ligand (**4**) is incorporated in the SAM. We assign the band at 1550 cm^{-1} to the two NH bends, the band at 1660 cm^{-1} to the two amide C=O stretches in the coupled ligand, and the band at 1733 cm^{-1} to the C=O stretch of residual carboxylic acid groups in **2**.

We have measured the increase in thickness ellipsometrically after coupling of **4** to the NHS esters of **2** in mixed SAMs (consisting of **1** and **2**). We can estimate the coupling yields (% yield) by dividing this observed increase in ellipsometric thickness (ΔT_{obs}) by the predicted increase in ellipsometric thickness (corresponding to quantitative coupling) ($\Delta T_{\text{predict}}$): i.e., % yield = $(\Delta T_{\text{obs}}/\Delta T_{\text{predict}})100$. The value of $\Delta T_{\text{predict}}$ can be estimated using eqs 2 and 3, where $\chi(\mathbf{2})_{\text{SAM}}$ is the mole fraction of **2** in a mixed SAM with thickness T_{mixedSAM} , ΔT_{2-1} is the difference in ellipsometric thickness ($\sim 21\text{ \AA}$) between a SAM

$$\Delta T_{\text{predict}} = \chi(\mathbf{2})_{\text{SAM}} \Delta T_{5-2} \quad (2)$$

$$\chi(\mathbf{2})_{\text{SAM}} = \frac{T_{\text{mixedSAM}} - T_1}{\Delta T_{2-1}} \quad (3)$$

consisting only of **2** ($\sim 41\text{ \AA}$)⁸ and a SAM consisting only of **1** (T_1 ; $\sim 20\text{ \AA}$), and ΔT_{5-2} is the difference in ellipsometric thickness ($\sim 20\text{ \AA}$) between a SAM consisting only of **5** (61 \AA) and a SAM consisting only of **2**. At values of $\chi(\mathbf{2})_{\text{SAM}} < 0.25$, the values of % yield are > 80 ; on the basis of these observations we infer that coupling of **4** to **2** occurs in high yield.⁶ This estimate is qualitatively compatible with the PIERS spectra (Figure 3).

We have previously described the binding of CA to SAMs of alkanethiolates on gold in which the thiol presenting the ligand (**5**) was synthesized separately.¹ The strategy of coupling of ligands to preformed SAMs made from **1** and **2** that present a common intermediate (the NHS ester of **2**) for coupling of ligands⁶ offers a number of advantages over the ex situ, independent synthesis of thiols presenting ligands: (a) organic synthesis is minimized—the only requirement is that the ligand contain at least one nucleophilic amino group; (b) the strategy permits the immobilization of delicate functional groups that might not be compatible with the manipulations required to isolate and purify thiols; (c) problems related to phase separation³⁰ of the ligand-presenting chains are reduced relative to mixed SAMs made from thiols with different hydrophobicities. The headgroup structures (ethylene glycol groups) of **1** and **2** are similar; this similarity tends to minimize phase separation.

We shall refer to the mole fraction of ligand in the SAM by $\chi(\mathbf{2}/\text{ASA})$ ($\text{ASA} = \mathbf{3}, \mathbf{4}$) rather than $\chi(\text{ASA})$ because the mole fraction of the ASA groups on the surface is not explicitly measured and because the yield on coupling the ASA groups to carboxylic groups at the surface is only an estimate. We assume that $\chi(\mathbf{2})_{\text{soln}} \sim \chi(\mathbf{2})_{\text{SAM}}$, since experimental evidence^{31–34} indicates that the composition of

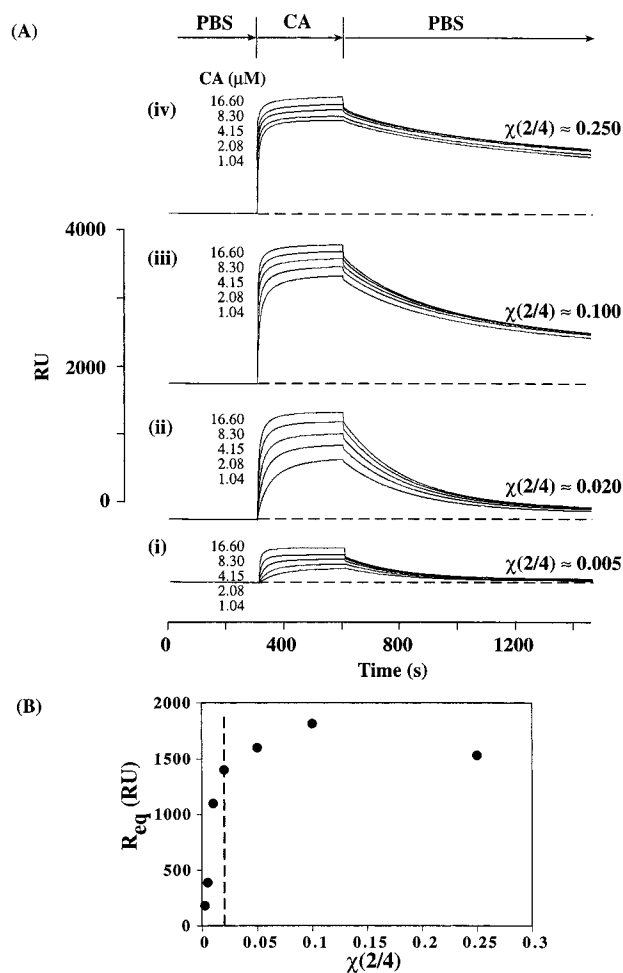


Figure 4. (A) Sensorgrams obtained by flowing CA (16.60, 8.30, 4.15, 2.08, and 1.04 μM) over surfaces presenting different mole fractions of **2** to which **4** had been covalently immobilized; (i) $\chi(\mathbf{2}/\mathbf{4}) \approx 0.005$, (ii) $\chi(\mathbf{2}/\mathbf{4}) \approx 0.020$, (iii) $\chi(\mathbf{2}/\mathbf{4}) \approx 0.100$, (iv) $\chi(\mathbf{2}/\mathbf{4}) \approx 0.250$. The buffer used was PBS. (B) Plot of R_{eq} (at $[\text{CA}] = 16.6\text{ }\mu\text{M}$) versus $\chi(\mathbf{2}/\mathbf{4})$. The dotted line [at $\chi(\mathbf{2}) \approx 0.02$] is a theoretical estimate of the mole fraction of ligand that is required to support the binding of a full monolayer of CA.

SAMs (for similar species) is well-described by the composition of the solution of thiols from which it is made.

Structure and Choice of ASA Ligand. To ensure that binding of CA to ASA was not hindered by proximity of the ligand to the “surface” of the SAM, we designed **2** to incorporate three more ethylene glycol groups than **1**. In initial experiments, we immobilized *p*-aminomethylbenzenesulfonamide (**3**) on the mixed SAMs consisting of **1** and activated **2**. At mole fractions of ASA groups that were comparable with the published report (using **5**),¹ we observed equilibrium response levels (R_{eq}) that were only 50% of those described earlier. Because the only difference between **3** (coupled to **2**) and **5** was the number of carbon atoms in the linker (methylene versus hexamethylene), we inferred that a longer linker would be preferable. The binding of CA to mixed SAMs presenting **4** (coupled to **2** by an amide bond) gave equilibrium response levels that were similar to that observed with mixed SAMs consisting of **1** and **5** (Figure 4).¹ These data suggest that binding of CA to ASA groups at a surface is dependent on the spacer length; the influence of spacer length on the binding of

(30) Folkers, J. P.; Laibinis, P. E.; Deutch, J.; Whitesides, G. M. *J. Phys. Chem.* **1994**, *98*, 563–571.

(31) Bain, C. D.; Biebuyck, H. A.; Whitesides, G. M. *Langmuir* **1989**, *5*, 723–727.

(32) Folkers, J. P.; Laibinis, P. E.; Whitesides, G. M. *Langmuir* **1992**, *8*, 1330–1341.

(33) Biebuyck, H. A.; Bain, C. D.; Whitesides, G. M. *Langmuir* **1994**, *10*, 1825–1831.

(34) Biebuyck, H. A.; Whitesides, G. M. *Langmuir* **1993**, *9*, 1766–1770.

proteins to ligands at surfaces has been demonstrated previously.^{21,35,36}

Influence of Density of ASA Groups on Binding Capacity of the Surface. We examined the binding of CA to mixed SAMs consisting of **1** and **2/4** as a function of $\chi(2/4)$. At values of $\chi(2/4)$ between 0 and 0.10, increasing $\chi(2/4)$ increased the steady-state response (R_{eq}) due to the binding of CA (Figure 4A, B). An increase in the density of ASA groups also resulted in an increase in the amount of CA that remained adsorbed at the end of the SPR experiment (at ~ 1450 s, see Figure 4A). The maximum value of R_{eq} (≈ 1820 RU, [CA] ≈ 16.6 μ M) was obtained at $\chi(2/4) \approx 0.10$. Increasing $\chi(2/4)$ further resulted in a decrease in the value of R_{eq} ; at $\chi(2/4) \approx 0.25$, $R_{eq} \approx 1500$ RU (Figure 4B).

Figure 5 is a cartoon showing the binding of CA to surfaces presenting ASA groups, at $\chi(2/4) \approx 0.005$ (Figure 5, top) and 0.10 (Figure 5, bottom). The figure is a view from the top that emphasizes the potential for adsorbed molecules of CA to shield ASA groups on the surface sterically at higher densities of ligand. The thiol molecules are shown arranged in a hexagonal pattern; the small open circles represent molecules of **1**, and the closed circles represent sites occupied by **2/4**. One adsorbed molecule of CA (radius ≈ 2.1 nm)^{9,37} covers approximately 61 molecules of coordinated alkanethiolates (see *Discussion*). When $\chi(2/4)$ is increased from 0.005 to 0.10 (a factor of 20), the number of molecules of CA that can be packed on the surface (without bumping into adjacent molecules of CA) is increased only two- to threefold. On the basis of the assumed cross-sectional area of CA (≈ 12.5 nm²), hexagonal packing, and a uniform distribution of ligands, the mole fraction of ASA required to observe the maximal amount of binding of CA is $\chi(2/4) \approx 0.02$. We observe an increase of ≈ 400 RU ($\sim 25\%$) in the value of R_{eq} as $\chi(2/4)$ is increased from ≈ 0.02 to 0.10; we attribute this increase to an underestimate of the amount of **2/4** on the surface, rather than to a surface density of protein higher than that predicted theoretically. The less-than-quantitative ($\sim 80\%$) yield in coupling of the ASA groups to the SAM is the major reason $\chi(2/4)$ might be lower than the values estimated from $\chi(2)$ in solution used to prepare the SAMs. The increased binding at $\chi(2/4) \approx 0.10$ could also be due to nonspecific adsorption of CA to the hydrophobic ASA groups, which could influence the kinetics of dissociation; the binding is $\sim 60\%$ and $\sim 90\%$ reversible at $\chi(2/4) \approx 0.10$ and $\chi(2/4) \approx 0.02$ respectively (Figure 4 A).

Kinetics of Binding of CA to ASA. We describe the kinetics of binding in three sections. We limit our discussion of kinetics to low mole fractions of ASA groups [$\chi(2/4) < 0.05$], where the binding of CA is highly reversible. The first section briefly summarizes general aspects of the kinetics of binding and the equations used to estimate $k_{on,obs}$ and $k_{off,obs}$. The second section discusses the influence of coverage of the surface by CA and density of ligand on $k_{off,obs}$; the third section describes the influence of these factors on $k_{on,obs}$.

(1) Equations of Rates of Dissociation and Association. We use k_{on} to refer to the rate constant that describes the second-order formation of the complex by association of CA and ASA, and k_{off} to describe its first-order dissociation; we use $k_{on,obs}$ and $k_{off,obs}$ (in these rate

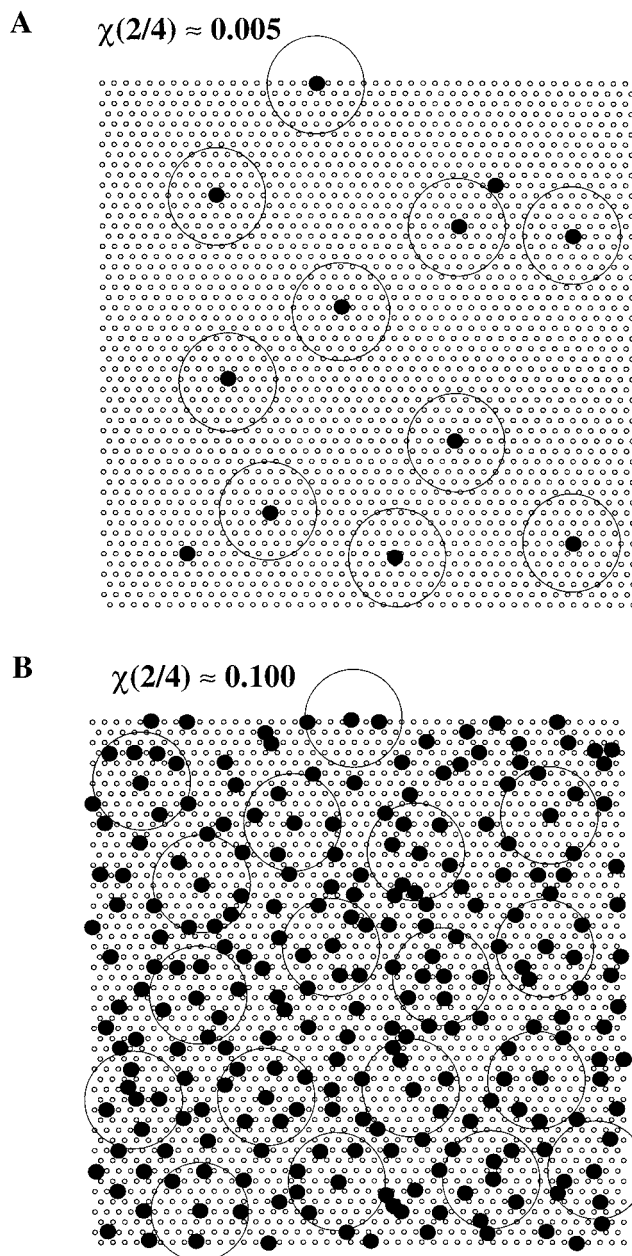


Figure 5. Schematic representation showing binding of CA (large open circles) to a randomized distribution of ligands (closed circles) on a surface at $\chi(2/4) \approx 0.005$ (A) and 0.10 (B). The surface shows hexagonally arranged alkanethiolate molecules (**1** or **2/4**) with a spacing of 5 Å; one adsorbed molecule of CA (radius ~ 2.1 nm, refs 9 and 37) covers ~ 60 of these molecules.

equations) when we express the surface density of the complex (CA·ASA) in terms of the SPR response, R_t .

We first discuss kinetics during the dissociation phase. The binding of CA to ASA was reversible at low densities of ligand [$\chi(2/4) \leq 0.05$]. The rate of dissociation of the ASA·CA complex, (CA·ASA)*, on the surface into free CA can be expressed by a first-order rate equation (eq 4): we calculated the value of $k_{off,obs}$ over the entire dissociation

$$d[\text{CA}\cdot\text{ASA}]^*/dt = dR_t/dt = -k_{off,obs} R_t \quad (4)$$

phase by fitting the exponential decay in the response to

(35) Ebato, H.; Herron, J. N.; Muller, W.; Okahata, Y.; Ringsdorf, H.; Suci, P. *Angew. Chem., Int. Ed. Engl.* **1992**, *31*, 1087–1090.

(36) Leckband, L. E.; Kuhl, T.; Wang, H. K.; Herron, J.; Muller, W.; Ringsdorf, H. *Biochemistry* **1995**, *34*, 11467–11478.

(37) Eriksson, A. E.; Jones, T. A.; Liljas, A. *Proteins: Struct., Funct., Genet.* **1988**, *4*, 274–282.

eq 5; eq 5 is the integrated form of

$$R_t = R_0 e^{-k_{\text{off}}(t-t_0)} \quad (5)$$

$$\ln(R_t/R_0) = -k_{\text{off,obs}}(t - t_0) \quad (6)$$

eq 4. In these equations, R_t is the response at time t , and R_0 is the response at the start time (t_0 , 600 s in the experiments described) from which $k_{\text{off,obs}}$ is calculated. Analysis of the dissociation curves using eqs 5 and 6 established that changes in the ligand density [$\chi(2/4) \leq 0.05$] and the concentration of CA (0.52–16.6 μM) did not significantly change $k_{\text{off,obs}}$. We estimated $k_{\text{off,obs}}$ to be $5.0 \pm 0.3 \times 10^{-3} \text{ s}^{-1}$.

The rate of formation of the ASA-CA complex, $(\text{CA} \cdot \text{ASA})^*$, on the surface can be expressed in terms of the change in response (R_t) during the association phase (eq 7). In

$$d[\text{CA} \cdot \text{ASA}]^*/dt = dR_t/dt = k_{\text{on}}[\text{CA}^{\text{soln}}][\text{ASA}]^* - k_{\text{off}}[\text{CA} \cdot \text{ASA}]^* \quad (7)$$

this equation, dR_t/dt is the rate of change of the SPR signal, $[\text{CA}^{\text{soln}}]$ is the concentration of CA in solution, and $[\text{ASA}]^*$ is the surface density of ASA groups. Equation 7 assumes that all ASA groups on the surface are available for binding with CA. This assumption is certainly incorrect for high values of $[\text{ASA}]^*$, when the surface is approaching saturation with CA; that is, when $[\text{CA} \cdot \text{ASA}]^*$ is approaching its maximum, close-packed value as a result of lateral interactions among the groups on the surface (see below). Because it is difficult to treat this case analytically, we continue our analysis by writing an equation in terms of the SPR response (eqs 8 and 9). In eq 8, R_{max} is the signal produced when $[\text{CA} \cdot \text{ASA}]^*$ is at its maximum density: that is, a close-packed monolayer. Rearranging eq 8 yields eq 9. The value

$$dR_t/dt = k_{\text{on,obs}}[\text{CA}^{\text{soln}}](R_{\text{max}} - R_t) - k_{\text{off,obs}}R_t \quad (8)$$

$$dR_t/dt = k_{\text{on,obs}}[\text{CA}^{\text{soln}}]R_{\text{max}} - (k_{\text{on,obs}}[\text{CA}^{\text{soln}}] + k_{\text{off,obs}})R_t \quad (9)$$

of $k_{\text{on,obs}}$ can be estimated from a slope of a plot of dR_t/dt versus R_t , using the known value of $[\text{CA}^{\text{soln}}]$ and the experimentally estimated value of $k_{\text{off,obs}}$. Plots of dR_t/dt versus R_t for binding of CA to ASA groups were not linear; by fitting data from the association phase over shorter intervals of time to eq 7, it became apparent that $k_{\text{on,obs}}$ decreased over the course of the association. To evaluate the influence of surface coverage on the rate constants of binding, we calculated instantaneous values of $k_{\text{on,obs}}$ and $k_{\text{off,obs}}$ and plotted their values against the estimated extent of coverage of the monolayer.

(2) Dissociation Phase: Dependence of $k_{\text{off,obs}}$ on Extent of Coverage of the Surface by CA and on Density of ASA Groups. The off-rate constants were calculated from the slope of plots of $\ln R_t/R_0$ versus time (eq 6), computed over periods of 1 s over the course of the dissociation (data were collected at 5 points per second). Figure 6 shows the time dependence of $k_{\text{off,obs}}$ at two concentrations of CA (16.6 and 1.04 μM) and at two different mole fractions of ligand [$\chi(2/4) \approx 0.020$ and 0.005], calculated over a period of 180 s (which corresponds to approximately 75% of the dissociation). Figure 6 establishes that $k_{\text{off,obs}}$ remained approximately constant at $\approx 5 \times 10^{-3} \text{ s}^{-1}$ with negligible (<5%) change during the process of dissociation of CA from the surface, and that it is

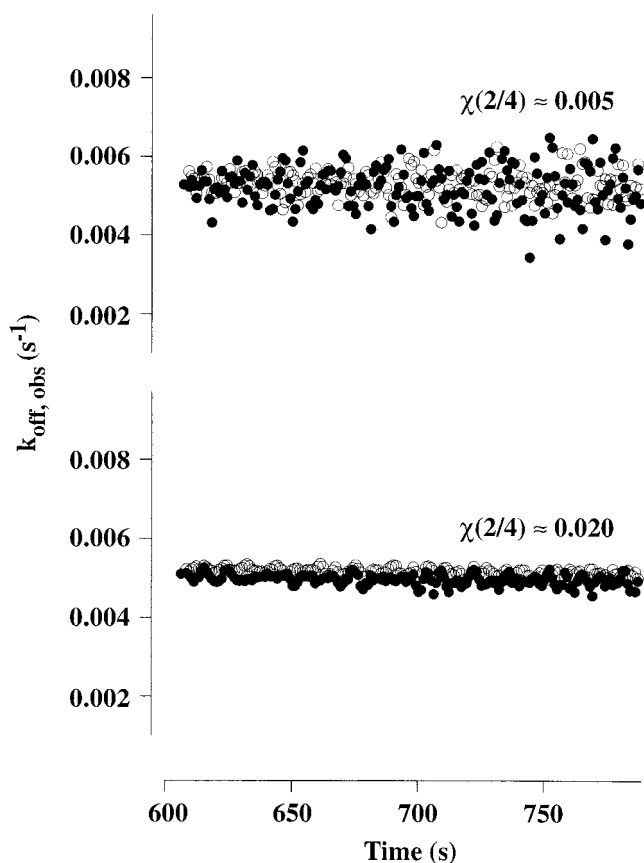


Figure 6. Analysis of the dissociation phase of the sensorgrams for $\chi(2/4) \approx 0.005$ and 0.10, at two concentrations of CA [16.6 μM (closed circles) and 1.04 μM (open circles)]. The figure shows that the value of k_{off} does not change significantly over the course of the dissociation.

independent of $\chi(2/4)$ over the range that was examined. We conclude that the density of ligand and the amount of CA bound to the surface (i.e., the extent of surface coverage by CA) do not influence the rate of dissociation, and hence, that lateral interactions (at low densities of ligand) have no significant effect on the rates of dissociation of proteins from surfaces.

(3) Association Phase: Dependence of $k_{\text{on,obs}}$ on Extent of Coverage of the Surface by CA. We also calculated $k_{\text{on,obs}}$ over short time intervals (1 s) throughout the association of CA to ASA on the surface. The basic procedure was as follows: (a) the value of the slope [equal to $(k_{\text{on,obs}}[\text{CA}^{\text{soln}}] + k_{\text{off,obs}})$] of a plot of dR_t/dt versus time was calculated over a period of 1 s (data were collected at 5 points per second) (eq 9); (b) The value of $k_{\text{on,obs}}$ was estimated using known values of the concentration of CA and the value of $k_{\text{off,obs}}$ (0.005 s^{-1}) determined from the dissociation phase. Figure 7A shows changes in $k_{\text{on,obs}}$ versus time [$\chi(2/4) \approx 0.02$] plotted over the first 60 s after the injection of CA over the surface. Even at the low density of ligand, there is a change in $k_{\text{on,obs}}$, with values ranging from $\approx 35 \times 10^3 \text{ M}^{-1} \text{ s}^{-1}$ to $4 \times 10^3 \text{ M}^{-1} \text{ s}^{-1}$, with the value decreasing with increasing coverage of the surface by CA. At very low values of $\chi(2/4)$ (~ 0.005), the value of $k_{\text{on,obs}}$ stays approximately constant at $\sim 35 \times 10^3 \text{ M}^{-1} \text{ s}^{-1}$ (Figure 7A, inset; also see *Discussion*).

We define P_t as the amount of protein adsorbed in nanograms per square millimeter; P_t can be estimated by dividing the observed response, R_t (in RU), by 1000.¹⁸ The fractional coverage of the surface by adsorbed CA can then be estimated from P_t/P_{max} where P_{max} is the maximum amount of protein that can be packed per square millimeter

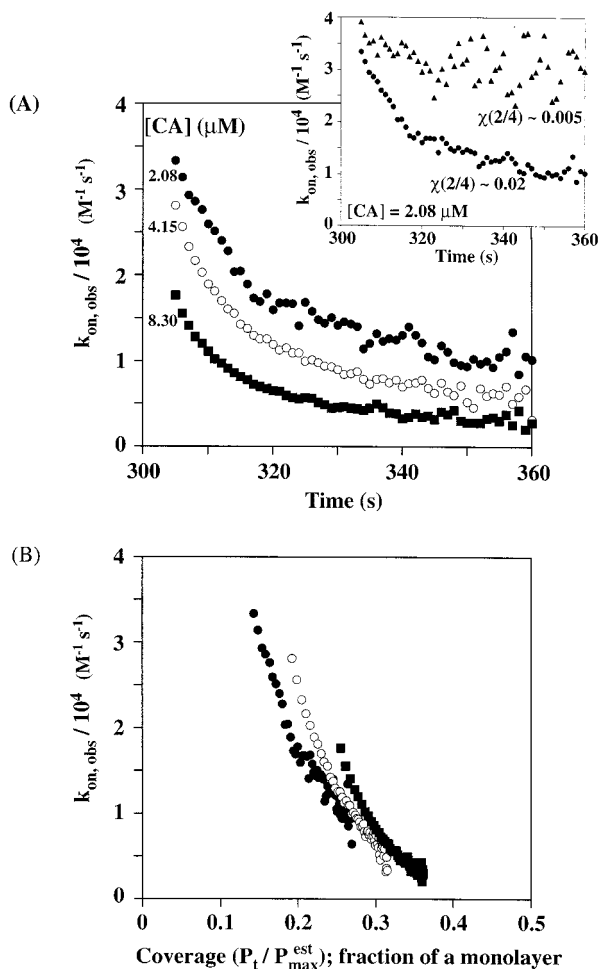


Figure 7. Analysis of the association phase of the sensorgrams for $(2/4) \sim 0.02$, at CA concentrations of 8.30, 4.15, and 2.08 μM . (A) $k_{\text{on,obs}}$ as a function of time; (B) $k_{\text{on,obs}}$ as a function of the estimated fraction of a close-packed monolayer coverage of CA. The inset shows the relative changes in $k_{\text{on,obs}}$ with time at $\chi(2/4) \approx 0.02$ and ≈ 0.005 .

on the surface of the monolayer. Equation 10 estimates the value of $P_{\text{max}} (P_{\text{max}}^{\text{est}})$: here, r is the radius

$$P_{\text{max}}^{\text{est}} \sim \frac{10^{21}}{\pi r^2 N_A} \text{MW} \quad (10)$$

(2.1 nm) of CA with a projected area of πr^2 in the plane of the monolayer, N_A is Avogadro's number, and MW is the molecular weight of CA (30 000). For CA, $P_{\text{max}}^{\text{est}} \sim 3.6 \text{ ng mm}^{-2}$ (equivalent to a response of $\approx 3600 \text{ RU}$).³⁸ Figure 7B is a plot of $k_{\text{on,obs}}$ versus $P_i/P_{\text{max}}^{\text{est}}$; the value of $k_{\text{on,obs}}$ decreases from $\sim 35 \times 10^3 \text{ M}^{-1} \text{ s}^{-1}$ to $\sim 4 \times 10^3 \text{ M}^{-1} \text{ s}^{-1}$ as $P_i/P_{\text{max}}^{\text{est}}$ increases from ~ 0.15 to ~ 0.35 . These data establish that the value of the observed rate constant of association decreases with the amount of protein adsorbed on the surface.

Discussion

We have used an experimental model system based on CA and immobilized ASA groups to explore deviations

(38) The maximum SPR signal we observe for binding of CA to ASA groups is only $\sim 1800 \text{ RU}$ (Figure 4). The maximum coverage that is expected with a mechanism for adsorption based on irreversible random adsorption is $\sim 55\%$; for reversible adsorption the maximum coverage is determined by the surface density of ligand and the dissociation constant (see Jin, X.; Talbot, J.; Wang, N.-H. L. *AIChE J.* **1994**, *40*, 1685–1696).

from ideal kinetic behavior. The most important observation is that at low densities of ASA groups where the binding of CA is highly reversible [e.g., at $\chi(2/4) \approx 0.02$], values of $k_{\text{on,obs}}$, but not of $k_{\text{off,obs}}$, decrease as the amount of CA adsorbed on the surface increases. One hypothesis that explains this result is that the decrease in $k_{\text{on,obs}}$ reflects lateral steric interactions between molecules in solution and those on the surface, and among molecules of CA adsorbed on the surface (Scheme 2, i, j).

The number of lattice sites, n , covered by a spherical protein molecule of radius r_{protein} , adsorbed on a hexagonal lattice characterized by a lattice vector of length a , is given by eq 11,³⁹ in which $k = r_{\text{protein}}/a$. For CA (radius 2.1 nm) adsorbed on a surface having lattice sites arranged with the geometry of an alkanethiolate SAM adsorbed on planar Au (111), $a \approx 5 \text{ \AA}$, $k \approx 4$, and $n \approx 61$. Although each molecule of CA physically covers

$$n = 3k(k + 1) + 1 \quad (11)$$

~ 60 lattice sites, there are additional *excluded* sites (shaded area in Figure 8) within a circle of radius $2k$; we refer to these sites as excluded (that is, not available to a molecule of CA in solution) because they would require the *centers* (but not the peripheries) of two molecules of adsorbed CA to approach distances less than their van der Waals surfaces. Taking this additional surface into account, an isolated adsorbed molecule of CA “shields” approximately 217 lattice sites.

A graph that shows the qualitative dependence of the fraction of unshielded ASA groups on the fraction of lattice sites with molecules of coordinated CA is shown in Figure 8. At low coverage of the surface with CA, the excluded areas of different molecules of protein on average do not overlap, and each molecule of adsorbed CA shields an area $A(2k)$ (or ~ 217 lattice sites). For uniformly distributed ASA ligands at $\chi(2/4) < 1/217 \sim 0.005$, the ASA ligands are sufficiently far apart that each molecule of adsorbed CA shields no more than one ASA ligand [and 216 (EG)₃OH groups]. Under these circumstances, the measured rate of association should be free of artifacts due to lateral steric effects, and therefore (in the absence of other effects) accurately represent the kinetics of the adsorption reaction at the interface. For binding of CA to mixed SAMs with $\chi(2/4) \approx 0.005$, the value of $k_{\text{on,obs}}$ ($\sim 3.5 \times 10^4 \text{ M}^{-1} \text{ s}^{-1}$) remains approximately constant (Figure 7A, inset). At intermediate coverages, the adsorbed molecules of CA are closer together and share their excluded areas: therefore, each protein shields on average *less* than $A(2k)$ lattice sites. The maximum coverage of CA at the surface (corresponding to no additional shielded area except that physically covered by CA) is achieved when molecules of CA are arranged in a close-packed hexagonal manner with their centers $2k$ away from each other. At this coverage, the fraction of lattice sites with molecules of coordinated CA is only 0.0016 (Figure 8). Experimentally, the maximum fractional coverage we observe for binding of CA to ASA groups {at $\chi(2/4) \sim 0.10$; $[\text{CA}] = 16.6 \mu\text{M}$ } is ~ 0.5 . The maximum coverage achieved for an interaction depends on the value of K_d and the values of k_{on} and k_{off} relative to the time scale of the experiment; fast on/off rates lead to greater lateral shuffling and therefore more efficient packing than binding that is irreversible or is characterized by slow on/off rates.³⁸

In Table 1 we list some reported values of K_d , k_{on} , and k_{off} for the interaction between CA and derivatives of benzenesulfonamide. Measurements based on affinity

(39) Stankowski, S. *Biochim. Biophys. Acta* **1984**, *777*, 167–182.

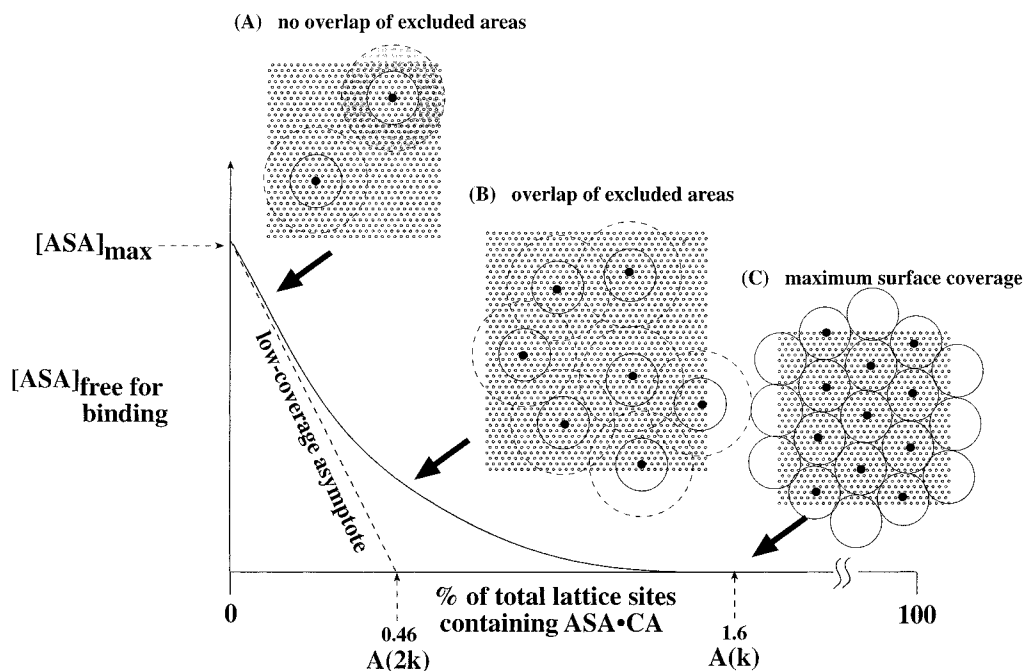


Figure 8. A curve showing the qualitative dependence of the fraction of ASA groups available for binding on the fraction of lattice sites (occupied by **1** and **2/4**) that contain coordinated molecules of CA (ASA·CA). Schematic views from the top showing adsorption of molecules of CA to SAMs presenting ASA groups, with the alkanethiolate molecules (**1** = small open circles; **2/4** = small closed circles) arranged on a hexagonal lattice, with a lattice vector of length a . We define: $k = r_{\text{protein}}/a$, where r_{protein} is the radius of CA; $k \approx 4$. Each molecule of adsorbed CA physically covers an area equal to $A(k)$, and “excludes” an additional area (shown as the shaded area) within a circle with area $A(2k)$. The consideration of this virtual shielded area helps define the limiting value of $\chi(\mathbf{2/4})$ below which no lateral effects should be observed. There are three basic regions in the curve. The first region (A) occurs at very low coverages of the surface by CA, in which on average there is no overlap of excluded areas by molecules of adsorbed CA (each molecule of CA shields an area equal to $A(2k)$, corresponding to 217 lattice sites). The second region (B) occurs at intermediate coverages, in which molecules of adsorbed CA share their excluded areas (molecules of CA shield areas between $A(2k)$ and $A(k)$, corresponding to 217 and 61 lattice sites respectively). The third region (C) of the curve refers to maximum coverage in which molecules of CA are adsorbed in a hexagonal close-packed manner [molecules of CA are separated by a center-to-center distance equal to $2k$, and shield an area equal to $A(k)$, corresponding to 61 lattice sites]; this arrangement is probably not achieved experimentally (see ref 38).

capillary electrophoresis,^{40–42} stopped flow fluorescence quenching,¹³ and the inhibition of enzymatic activity (CO₂ hydration)⁴³ are all solution-based and therefore free of some of the artifacts (e.g., lateral effects) inherent to measurements of binding of biomolecules to surfaces. Analysis of SPR data is complicated (see below) but offers the convenience of direct monitoring of rate constants for both association and dissociation, and for equilibrium binding.

We have hypothesized that lateral interactions between molecules of CA and ASA groups and among molecules of CA are responsible for the decrease we observed in $k_{\text{on,obs}}$. We also need to consider other possible origins for this decrease and discuss some possibilities below, as outlined before in Scheme 2. The arguments we present pertain only to low mole-fractions of $\chi(\mathbf{2/4})$; binding of CA to these surfaces is reversible within the time scale of the experiment and is described by a single observed rate constant of dissociation. For many of the reasons described below, it would be difficult to distinguish between these mechanisms and lateral steric effects at high surface densities of ASA groups.

(1) Partitioning of Ligand (b) and Adsorbed CA (g) Between Solution and Ethylene Glycol Layer.

(40) Colton, I. J.; Carbeck, J. D.; Rao, J.; Whitesides, G. M. *Electrophoresis* **1998**, *19*, 367–382.

(41) Gomez, F. A.; Avila, L. Z.; Chu, Y. H.; Whitesides, G. M. *Anal. Chem.* **1994**, *66*, 1785–1791.

(42) Avila, L. Z.; Chu, Y.-H.; Blossley, E. C.; Whitesides, G. M. *J. Med. Chem.* **1993**, *36*, 126–133.

(43) Maren, T. H. *Mol. Pharmacol.* **1992**, *41*, 419–426.

The (EG)₃ groups at the termini of the SAM form a packed layer⁴⁴ that is sufficiently dense that molecules of protein would not be able to penetrate it; although interaction of protein with the outer layer is, in principle, possible, it is unlikely because proteins do not adsorb on (EG)_n layers.⁸ There is, however, probably enough free volume in the (EG)₃ layer that a small group such as ASA might partition into it. If adsorption of CA on the surface of the SAM resulted in a change in the structure and the free volume of the (EG)₃ layer, this change might be reflected in a change in the availability of remaining ASA groups. Because the density of ASA groups at the surface influences $k_{\text{on,obs}}$, perturbations in the availability of ASA groups for binding could lead to a change in $k_{\text{on,obs}}$. In the absence of any experimental evidence regarding differences in the partitioning of ASA groups into the (EG)₃ layer with and without adsorbed CA, we cannot rule out the possible influence of this mechanism on $k_{\text{on,obs}}$.

(2) Nonbiospecific Interaction of CA with ASA Ligands at the Surface (e). Figure 4 shows that binding is less reversible (or is kinetically slower) at higher densities of ASA ligands relative to binding at lower densities. We assume that increasing irreversibility reflects secondary, nonbiospecific binding between CA and proximal hydrophobic ASA ligands. Lateral interactions between CA and ASA groups would lower the fraction of those ASA groups available for biospecific interaction with additional molecules of CA, or increase the activation

(44) Harder, P.; Grunze, M.; Dahint, R.; Whitesides, G. M.; Laibinis, P. E. *J. Phys. Chem. B* **1998**, *102*, 426–436.

energy (or lower the free energy of association) for biospecific binding by requiring the initial dissociation of nonspecific complexes. Because this type of lateral interaction will parallel lateral interactions between molecules of CA, it is difficult to distinguish one from the other; therefore we limit our kinetic analysis only to surfaces presenting low surface densities of ASA groups where $k_{\text{off,obs}}$ remains constant over the dissociation phase.

(3) Changes in pK_a of ASA Group Due to Changes in Local Environment during Binding of CA (f). The binding of CA to the ASA groups results in the expulsion of water molecules from the surface of the SAM; this exchange of water molecules for molecules of protein may result in a local decrease in the dielectric constant of the medium at the interface. On the basis of the Born model of solvation of ions, an ion has a more favorable free energy of solvation in a medium of high dielectric constant than in a medium of low dielectric constant;⁴⁵ thus, in principle, the ASA group should be less prone to ionization (deprotonation) in a medium of low dielectric constant consisting of molecules of adsorbed protein than it is in aqueous buffer (f). To determine if the total charge of the CA·ASA complex is the same in the absence of ASA, we measured the electrophoretic mobility of CA by capillary electrophoresis. We observed no change in the electrophoretic mobility of CA (relative to 4-methoxybenzyl alcohol as a neutral marker) when the buffer also contained the ASA ligand **6** (at $\sim 700 \mu\text{M}$).⁴⁶ Therefore, the total charge of the CA·ASA complex is the same as that of CA in the absence of ASA,^{40,47} which implies that the change in the free energy of deprotonation of the ASA group is irrelevant; the change in free energy of deprotonation of the ASA group is compensated by the change in the free energy of protonation of the hydroxyl ion that is displaced (eq 1). Moreover, even if there were a change in the charge of CA upon binding to ASA, changes in the pK_a of the ASA group would also affect k_{off} , which is contrary to experimental observation.

(4) Mass Transport Limited Association and Dissociation (d). An increase in $k_{\text{on,obs}}$ at lower densities of ligand on the surface can indicate that binding is limited by mass transport.²⁴ We first consider a theoretical analysis of the influence of mass transport on the observed rates of association and dissociation using an approach adapted from Glaser.²⁴ The driving force for diffusion, and therefore the flux, j_d (in moles per second per square meter), is proportional to the difference in the concentration of the receptor in the bulk solution, c_o (in moles per liter) and the concentration of the free receptor at the surface, c_{fs} (in moles per liter) (eq 12). Mass transport will influence the observed rates of association and dissociation whenever c_{fs} differs from c_o . The driving force for binding, and therefore the flux, j_b (in moles per second per square meter), is proportional to the difference between c_{fs} and the concentration of receptor in solution that is in equilibrium with ligand on the surface, c_{eq} (in moles per liter) (eq 13). The proportionality constants in eqs 12 and 13 that relate fluxes to differences in concentrations are referred to as Onsager coefficients: L_m (in meters per second) is the Onsager coefficient of mass transport; L_r (in meters per second) is the Onsager coefficient of reaction flux. Conservation of mass requires that $j_b = -j_d$: when $L_m \gg L_r$ the flux is limited by j_b and the observed rates of association

and dissociation reflect the intrinsic kinetics of binding; when $L_r \gg L_m$ the flux is limited by j_d and the observed rates reflect the effects of mass transport.

$$j_d = -L_m(c_o - c_{\text{fs}}) \quad (12)$$

$$j_b = L_r(c_{\text{fs}} - c_{\text{eq}}) \quad (13)$$

An estimate of the effects of mass transport requires an estimate of the values of the Onsager coefficients, L_m and L_r . The value of L_m can be estimated from Fick's first law, given in eq 14, where D is the coefficient of diffusion ($\approx 1 \times 10^{-10} \text{ m}^2 \text{ s}^{-1}$, for CA⁴⁸) and $\partial c/\partial z$ is the value of the gradient of concentration, which, in turn, may be estimated from the values of c_{fs} , c_o , and the thickness of the diffusion boundary layer, d . One estimate of d , on the basis of the work of Leveque (ref 16 of the paper by Glaser), is given in eq 15, where \dot{V} is the rate of flow ($0.3 \mu\text{L s}^{-1}$); h , w , and l are the height ($50 \mu\text{m}$), width ($300 \mu\text{m}$), and length ($800 \mu\text{m}$), respectively, of the flow cell. The value of L_m using this estimate of d is expressed in eq 16. We estimate $L_m \approx 1.5 \times 10^{-5} \text{ m s}^{-1}$.

$$j_d = -D \frac{\partial c}{\partial z} \approx -D \frac{(c_o - c_{\text{fs}})}{d} \quad (14)$$

$$d \approx \sqrt{\frac{D \dot{V}^2 w l}{f}} \quad (15)$$

$$L_m \approx \sqrt[3]{\frac{D^2 f}{h^2 w l}} \quad (16)$$

The value of L_r is estimated from the expression for j_b given in eq 17, where g_b (in moles per square meter) is the density of ligands on the surface that are bound to receptors, g_{fr} (in moles per square meter) is the density of free ligands on the surface, and k_{on} and k_{off} are the rate constants for association and dissociation, respectively. Factoring out the term $k_{\text{on}} g_{\text{fr}}$, and recognizing that $k_{\text{off}} g_b/k_{\text{on}} g_{\text{fr}} = c_{\text{eq}}$, gives eq 18, yielding the expression for L_r (eq 19).

$$j_b = \frac{\partial g_b}{\partial t} = k_{\text{on}} c_{\text{fs}} g_{\text{fr}} - k_{\text{off}} g_b \quad (17)$$

$$j_b = k_{\text{on}} g_{\text{fr}} (c_{\text{fs}} - k_{\text{off}} g_b/k_{\text{on}} g_{\text{fr}}) = k_{\text{on}} g_{\text{fr}} (c_{\text{fs}} - c_{\text{eq}}) \quad (18)$$

$$L_r = k_{\text{on}} g_{\text{fr}} \quad (19)$$

Equation 19 implies that mass transport is most prominent at the beginning of the association phase and toward the end of the dissociation phase when the density of unoccupied sites (g_{fr}) is highest. We next estimate L_r at the beginning of the association phase when the value of L_r is a maximum. At this stage, the observed rate of binding is most limited by mass transport; the estimation of the maximum value of L_r provides the lower limit of L_m/L_r .

We first estimate the density of ASA groups at the surface on the basis of the observed amount of CA that adsorbs. When the mole fraction of ASA groups at the surface is low, it is possible to estimate the molar density of ASA groups (in moles per square meter) at the surface by calculating the molar density of adsorbed CA (in moles per square meter): that is, $1 \text{ RU} \sim 10^{-6}/\text{MW}$ of CA (in moles per square meter; MW is the molecular weight of

(45) Israelachvili, J. *Intermolecular and Surface Forces*; Academic Press: San Diego, 1992.

(46) Jain, A.; Huang, S. G.; Whitesides, G. M. *J. Am. Chem. Soc.* **1994**, *116*, 5057–5062.

(47) Mammen, M.; Colton, I. J.; Carbeck, J. D.; Bradley, R.; Whitesides, G. M. *Anal. Chem.* **1997**, *69*, 2165–2170.

(48) *CRC Handbook of Biochemistry*; CRC Press: Boca Raton, FL, 1970.

CA, $\sim 30\,000$). For example, at $\chi(2/4) \approx 0.005$, the maximal binding capacity of the surface is ≈ 400 RU; this number corresponds to a molar density (for CA) of 1.3×10^{-8} mol m^{-2} . If we assume that maximal binding corresponds to binding of one molecule of CA to every ASA ligand (1:1 binding), a reasonable assumption at $\chi(2/4) \approx 0.005$, the total density of ASA ligands at the surface is approximately 1.3×10^{-8} mol m^{-2} . Substituting this number and the value of $k_{on,obs}$ ($\approx 3.5 \times 10^4$ M $^{-1}$ s $^{-1}$) in eq 19 allows us to calculate the maximum value of L_r at any mole fraction of ligand. Assuming that the molar density of ligands (in moles per square meter) is proportional to the mole fraction of the ligand, we calculate: $L_r \approx 4.55 \times 10^{-7}$ mol m^{-2} at $\chi(2/4) \approx 0.005$; $L_r \approx 18.2 \times 10^{-7}$ mol m^{-2} at $\chi(2/4) \approx 0.02$.

At the beginning of the association, at $\chi(2/4) \approx 0.02$, the value of $L_m/L_r \sim 9$, and hence the observed kinetics is not limited by mass transport. The value of $k_{on,obs}$ decreases with coverage of the surface by CA at this mole fraction (Figure 7). We conclude that this decrease is not due to the effects of mass transport. We also note that a decrease in $k_{on,obs}$ with coverage of the surface by CA is opposite to the expected increase in $k_{on,obs}$ with coverage that is expected if mass transport effects were dominant (eq 7, 19).

(i) *Variations in Flow Rate.* We do not observe an increase in the rates of association and dissociation by increasing the flow rate (between 0.08 and 1.7 $\mu\text{L s}^{-1}$, which results in a change in L_m of 9.6×10^{-6} ms $^{-1}$ to 2.7×10^{-5} ms $^{-1}$) (eq 16).

(ii) *Analysis of Dissociation Phase.* We do not observe any significant decrease in $k_{off,obs}$ during the course of the dissociation. If the interaction were limited by mass transport, we would have expected a decrease in the observed value of $k_{off,obs}$ over the course of the dissociation due to rebinding of molecules of CA to the increasing number of free ASA groups at the surface. Plots of k_{off} versus time (Figure 6) show less than a 5% decrease in its value.

(iii) *Analysis of Dissociation Phase: Addition of Soluble Ligand.* It is possible to infer effects due to mass transport experimentally by the addition of soluble ligand during the dissociation phase.²⁴ This experimental technique is the most commonly used method for detecting interactions limited by mass transport, because it is more sensitive to the effects of mass transport than the method of variations in flow rate (L_m has cube root dependence on f , eq 16).^{24,25} If the interaction is limited by mass transport, the presence of soluble ligand leads to faster rates of dissociation. The increase is due to the capture of the dissociated molecules of analyte near the surface; this competitive interaction prevents rebinding to the surface. Figure 9 shows the dissociation phases from sensorgrams [at $\chi(2/4) \approx 0.02$] obtained in the presence and absence of soluble ligand (100 μM *p*-carboxybenzenesulfonamide, $K_d \approx 2.2$ μM). We observe that the rate of dissociation of CA is unaffected by the presence of *p*-carboxybenzenesulfonamide in the buffer. These data establish that the interaction of CA and ASA is not limited by mass transport at low surface densities of ASA groups.

Conclusion

The binding of CA to mixed SAMs presenting ASA groups was chosen as a model system to study lateral steric effects. At low surface densities of ASA groups, this model system is not complicated by issues such as nonspecific binding, divalency, irreversible adsorption, and mass transport. We observed that the value of the association constant ($k_{on,obs}$) decreased ~ 10 -fold as the

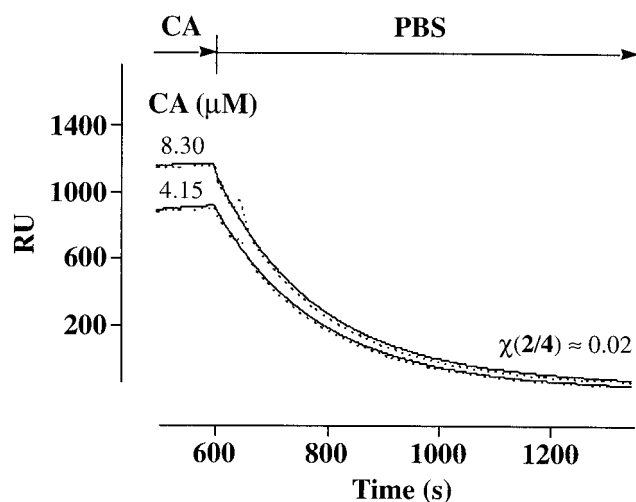


Figure 9. Sensorgrams showing the dissociation of CA from the surface, with (---) and without (—) *p*-carboxybenzenesulfonamide (100 μM) in the buffer (PBS). This experiment was carried out using a SAM with $\chi(2/4) \approx 0.02$.

fractional coverage of the monolayer by CA increased from 0.15 to 0.35; we did not observe any corresponding decrease in the value of the dissociation constant ($k_{off,obs}$). We hypothesize that these observations reflect lateral steric effects.

One explanation of this effect is that each molecule of biospecifically adsorbed CA shields proximal ASA ligands and prevents their binding to incoming molecules of CA; this shielding decreases the concentration of free ASA groups and results in an apparent decrease in the value of the association constant. The effect would thus be largely a statistical effect: the available surface density of ASA ligands decreases during adsorption of CA substantially more rapidly than the increase in the surface density of CA, provided the surface density of ASA groups is high (but not too high to lead to additional complications). Although this explanation is compatible with the experimental data, and although we chose this system to study lateral effects because of its apparent simplicity, we cannot eliminate some other possibilities that could also account for these observations: lateral interactions of ASA groups with themselves or with bound molecules of CA, partitioning of ASA groups into the (EG) $_n$ layer, etc.

This study illuminates some of the complications that are inherent in studies of the kinetics of biospecific binding of proteins to surfaces. The work also demonstrates the advantages of using mixed SAMs of alkanethiolates on gold-presenting ligands and (EG) $_3$ OH groups for studies of fundamental aspects of biomolecular recognition at surfaces. Even with this structurally well-defined system, the complexities in the analysis are substantial. We suspect that a corresponding analysis with an experimental system based on dextran gels would be intractably difficult, because it introduces yet further issues in partitioning and mass transport.

Experimental Section

Materials. Bovine CA II was obtained from Worthington. Sodium dodecyl sulfate (SDS) was obtained from BioRad. NHS, EDC, and *p*-aminomethylbenzenesulfonamide were purchased from Aldrich. Compounds **1** and **6** were prepared as described previously.^{7,8,46}

Preparation of Gold Substrates Presenting Mixed SAMs. Gold substrates were prepared by evaporating thin films of titanium (1.5 nm, to promote adhesion of gold to glass) and gold (40 nm) onto glass coverslips (0.2 mm, no. 2, Corning, used as

obtained). Stock solutions of thiols **1** and **2** (2 mM in ethanol) were combined in different ratios in glass scintillation vials. The gold substrates were incubated in the solutions of thiols for 8–12 h, rinsed with ethanol, dried under a stream of nitrogen, glued into cartridges (commercial CM5 cartridges from BIAcore from which the entire gold-coated glass slide bearing the dextran is peeled off with a razor blade), and then docked into the BIAcore instrument. These substrates were used within 24 h. For repetitions of experiments, fresh solutions of mixed thiols were made and used within 24 h.

Buffers and Solutions. All solutions were passed through 0.22- μm filters (Acrodisc, HT Tuffryn membrane). PBS (10 mM phosphate, 138 mM NaCl, and 2.7 mM KCl) was prepared in distilled, deionized water. Solutions of NHS (0.10 M) and EDC (0.4 M) were prepared in distilled, deionized water *immediately* before use and mixed (1:1) in the BIAcore 1000 instrument just before activation of the surface. Solutions of CA used in the binding experiments were prepared in PBS. Solutions of the benzenesulfonamide ligands **3** (saturated solution, pH 8.0) and **4** (2 mg mL⁻¹, pH 8.0) were prepared in 25 mM phosphate buffer.

Ellipsometry. A commercially available ellipsometer (AutoEL I, Rudolph, Inc.) using a He–Ne laser ($\lambda = 632.8$ nm) was used for all experiments. Gold-coated silicon substrates were prepared by evaporating titanium (2.5 nm) and gold (200 nm) on silicon substrates (Silicon Sense). These substrates were cut into squares ~ 1.5 cm in length, washed with distilled water and EtOH, and dried under a stream of nitrogen. After determining the optical constants for the substrates, they were immersed in solutions containing mixtures of **1** and **2** or **1** and **5** for a period of 12 h. Ellipsometric thicknesses for these substrates were then determined using the previously measured values of optical constants. Immobilization of **4** to mixed SAMs of **1** and **2** was accomplished by sequentially immersing the substrates in aqueous solutions containing NHS (0.05 M) and EDC (0.20 M) for 7 min, a solution of **4** (2 mg mL⁻¹; 25 mM pH 8 phosphate buffer) for 7 min, and finally pH 8.6 phosphate buffer (25 mM) for 20 min. Between each immersion, the substrates were washed with PBS for ≈ 1 min. After coupling, the substrates were washed with distilled water and ethanol and dried under a stream of nitrogen. The ellipsometric thickness of these substrates was then measured to estimate the increase in thickness after coupling to **4**.

PIERS. PIERS spectra were obtained in single reflection mode using a dry, nitrogen-purged Digilab Fourier transform infrared spectrometer (BioRad, Cambridge). The p-polarized light was incident at 80° relative to the surface normal of the substrate and a mercury–cadmium–telluride detector cooled with liquid nitrogen was used to detect the reflected light. A bare gold substrate similar to the one described for the ellipsometric measurements was used as a reference. Typically, 1024 scans were averaged to obtain spectra shown in this paper. The coupling procedure was similar to that described for the ellipsometric measurements.

Capillary Electrophoresis (CE). Electropherograms were collected using a Beckman P/ACE 5500 system for CE. The general conditions used were: operating voltage of 15 kV; temperature, 25 °C (maintained by liquid cooling); total length of capillary, 47 cm; inner diameter, 50 μm . The buffer used for electrophoresis was 25 mM Tris and 192 mM Gly (pH 7.4), with or without the ligand **6** dissolved in the buffer (694 μM). The capillary was flushed with 0.1 N NaOH, distilled water, and electrophoresis buffer for 2 min before each experiment.

Procedure for Immobilization of ASA Ligands for Studies by SPR. The BIAcore 1000 is equipped with an autosampler and can be programmed for automatic handling of samples. All operations including mixing of solutions, activation

of the surface, coupling by peptide bond-forming reactions, and quenching of unreacted active ester groups were carried out automatically and sequentially using programs for immobilization of ligands to surfaces. A flow rate of 5 $\mu\text{L min}^{-1}$ was used throughout the immobilization.

Vials containing solutions of NHS (0.05 M in water), EDC (0.20 M in water), the ligand (**3**, **4**) (6.5 mM in pH 8 phosphate buffer), and pH 8.6 phosphate buffer were put in separate positions of the autosampler tray. Equal volumes of the NHS and EDC solutions were combined in an empty vial in the autosampler tray by using the DILUTE command (described in the instruction manual for the BIAcore 1000).

The surface of the SAM was first equilibrated with PBS. Activation of the surface was achieved by transformation of the carboxylic acid groups on the surface into NHS esters by passing the solution containing the mixture of NHS and EDC over the surface for 7 min. The system was then returned to PBS (2 min) and the solution of the ligand (**3**, **4**) was passed over the surface (7 min), resulting in amide bond formation by displacement of the NHS esters. The system was returned to PBS and excess NHS esters were deactivated by a 20-min wash with pH 8.6 phosphate buffer.

Measuring Binding of CA to ASA Groups by SPR. The adsorption of CA to the surface was measured by allowing a solution of buffer (PBS) to flow through the cell for 5 min, substituting a solution of CA (at concentrations of 16.6, 8.30, 4.15, 2.08, 1.04, and 0.52 μM) in the same buffer for 5 min, and then replacing it with the original buffer for 15 min (Figure 1). After each binding experiment, residual amounts of adsorbed CA were removed by flowing a solution of detergent (SDS, 10 mg mL⁻¹ in PBS) over the surface at a flow rate of 10 $\mu\text{L min}^{-1}$ for 5 min.⁴⁹

11-[19-Carboxymethylhexa(ethylene glycol)]undec-1-ylthiol (2**).** A solution of AcS(CH₂)₁₁O[(CH₂)₂O]₆CH₂CO₂Me (200 mg, 0.34 mmol) in MeOH (2 mL) and a solution of LiOH (35 mg) in MeOH (8 mL), both separately purged with Ar for 30 min, were mixed together. After stirring under argon for 12 h at room temperature, acetic acid (180 μL) was added by syringe to neutralize the reaction mixture. The solvent was evaporated and the crude residue was purified by flash chromatography (SiO₂, 88:10:2 chloroform/methanol/acetic acid), giving **2** (105 mg, 58%). ¹H NMR (300 MHz, acetone-*d*₆): 4.00 (s, 2H), 3.7–3.5 (m, 24 H), 3.42 (t, *J* = 6.5 Hz, 2H), 2.50 (dt, *J* = 7.8, 7.0 Hz, 2H), 1.67 (t, *J* = 7.8 Hz, 1H), 1.6–1.3 (br s, 18 H). HRMS (FAB⁺): 549.3090 [calcd for C₂₅H₄₉O₉SNa (M + Na): 549.3073].

(6-Aminohexamethylene)-4-sulfamoylbenzamide (4**).** The benzenesulfonamide ligand **5** was prepared by coupling the NHS ester of 4-carboxybenzenesulfonamide with mono *t*-Boc-protected 1,6-hexanediamine, followed by deprotection with 50% trifluoroacetic acid in CH₂Cl₂ (2 h, room temperature). ¹H NMR (400 MHz, acetone-*d*₆): 8.43 (br, 2H), 8.19 (t, *J* = 5.4, 1H), 8.01 (d, *J* = 8.2, 2H), 7.94 (d, *J* = 8.2, 2H), 6.82 (br s, 2H), 3.81 (m, 2H), 3.41 (m, 2H), 1.82 (m, 2H), 1.62 (m, 2H), 1.45 (m, 4H). MS (FAB): 300 (M⁺, calcd for C₁₃H₂₂N₃O₃S).

Acknowledgment. Financial support from the National Institutes of Health (GM 30367 and a postdoctoral fellowship to L.I.) and DARPA/SPAWAR is gratefully acknowledged. We thank Professor Paul Laibinis (MIT) for use of the FTIR instrument in his laboratories.

LA9815650

(49) Sigal, G. B.; Mrksich, M.; Whitesides, G. M. *Langmuir* **1997**, *13*, 2749–2755.